Redox-dependent Structural Origin of the Temperature Threshold and Sensitivity in the TRPV3 Thermometer

Guangyu Wang (gary.wang10@gmail.com)
University of California Davis https://orcid.org/0000-0002-5581-6926

Research Article

Keywords: graph theory, hairpin thermodynamics, ion channel, non-covalent interaction, redox-dependence, temperature sensitivity, threshold, topological gating loop

Posted Date: April 19th, 2022

DOI: https://doi.org/10.21203/rs.3.rs-1556082/v4

Abstract

The DNA hairpin with a limited size is sensitive to temperature. However, it is unclear if thermosensitive TRP channels also use temperature-dependent hairpin sizes to govern their activation temperature thresholds and sensitivity. Here, graph theory, together with redox- and state-dependent cryo-electron microscopy structures of TRPV3 with or without an agonist at different temperatures, was to test this hypothesis. The results showed that the largest hairpin topological loop size and a change in the total hairpin sizes along the channel gating pathway control the temperature threshold and sensitivity, respectively. This size-dependent hairpin thermodynamics may mediate the thermal activity of biological macromolecules.

1. Introduction

The transient receptor potential (TRP) channels can be gated by both physical and chemical stimuli to conduct cations. Among 28 mammalian members in the TRP superfamily, eleven ones are thermosensitive through a variety of TRP channel families including TRPV (vanilloid), TRPM (melastatin), TRPC (canonical), and TRPA (ankyrin). Their temperature thresholds for activation range from noxious cold, cold, warm to noxious hot. Specifically, TRPV1 (>42 °C), TRPV2 (>52 °C), TRPV3 (>32–39 °C), TRPV4 (>25–35 °C), TRPM2, TRPM3, TRPM4, and TRPM5 are involved in warm to hot sensation. In contrast, TRPA1 (<17 °C) or TRPM8 (<20–28 °C) and TRPC5 (<25-37 °C) are sensitive to cold and cool temperatures. These thermosensitive TRP channels also have a high temperature coefficient or Q_{10} compared to non-temperature-sensitive ion channels [1-16]. However, the origin of both the temperature threshold and the sensitivity is unknown.

A critical clue comes from a DNA hairpin thermal biosensor. Its hairpin sizes within 10-30 bases in the loops produce temperature thresholds in the range of those thermosensitive TRP channels. The larger hairpin size has the lower threshold. Its melting curve also has a characteristic slope as the temperature sensitivity (Q_{10}=1.7-4) [17]. Therefore, it is exciting to ask if the temperature-dependent largest hairpin size along the gating pathway of thermosensitive TRP channels initiates an activation threshold while a change in the total hairpin sizes between closed and open states of a single channel controls Q_{10}. The recent state- and redox-dependent cryo-electron microscopy (cryo-EM) structures of mTRPV3 at a threshold 42□C may provide an opportunity to examine the hypothesis [18]. In addition, mTRPV3 undergoes sensitization upon successive heat stimuli while TRPV1, 2 and 4 channels desensitize [7, 19-21]. Thus, the sensitized mTRPV3 may be an intermediate underlying the thermo-gated activation mechanism.

TRPV3 has a high temperature sensitivity (Q_{10}=27) [18]. It is mainly expressed in skin keratinocytes and oral and nasal epithelia, mediating thermal reception and pain sensation [5-6]. Like other TRPV channels, TRPV3 is a homotetramer. Each monomer has S1-S6 as transmembrane domain (TMD) and a large intracellular amino- (N-) terminal as ankyrin repeat domain (ARD). S1-S4 form a voltage-sensor-like domain (VSLD) while S5-S6 and the pore helix and two pore loops are folded as a pore domain. Both the

VSLD and the pore domain are swapped via an S4–S5 linker. The TRP helices, which are almost parallel to the membrane, interact with both the skirt ARD and the TMD. Several lipid sites were also found in their interfaces. The pre-S1 domain, together with the carboxy- (C-) terminal loop domain, couples TMD with ARD. The residues ^{638}GLGD^{641} in the P-loop-extended region line the selectivity filter to permeate partially hydrated Na^+ , K^+ or Ca^{2+} ions but not to function as a upper gate. In contrast, the narrowest pore constriction around M677 on S6 may act as a lower gate. When TRPV3 is opened by the common agonist 2-aminoethoxydiphenyl borate (2-APB) of thermosensitive TRP channels, mostly hydrophobic residues in the pore turn into primarily hydrophilic and negatively-charged residues with α-to-π-helix transitions in S6. In the meanwhile, the S6 helices become longer by two helical turns with two helical turns shorter and a ~20° rotation in the TRP against the membrane plane [22-23]. In this regard, the cryo-EM structures of mTRPV3 with or without 2-APB at low temperature can serve as ideal controls to test the above hypothesis.

2. Results

2.1 The Non-covalent Interactions Form Multiple Hairpin Topological Loops along the Gating Pathway of Oxidized mTRPV3 at 42□C

C612 and C619 in the outer pore of mTRPV3 can form a disulfide bond upon oxidization [18]. In the closed state at 42□C, the diversity of non-covalent interactions between amino acid side chains in oxidized mTRPV3 can produce multiple hairpin topological loops along the gating pathway from D396 in the pre-S1 domain to K505 in the TRP domain. First, salt bridges are present between several charged pairs. For example, R416 on pre-S1 and D519 in the S2-S3 linker, K432 on pre-S1 and E704 in the TRP domain or D396 on pre-S1, D586 and K589 on S5, E631 and K634 on the pore helix, E682 on S6 and K686 in the TRP domain, E687 and K690, E689 and R693, R698 and E702 in the TRP domain (Figure 1).

Second, p-p interactions appear between several pairing aromatic residues. They include: F441 on S1 and W433 on pre-S1 or Y565 on S4, F445 and F449 on S1 or Y565 on S4, Y448 on S1 and F526 on S3 or Y565 on S4, W493 and F489 on S2 or F447 or Y451 on S1, F526 on S3 and Y564 on S4, Y540 on S3 and Y547 on S4, Y564 and Y565 on S4, F590 and Y594 on S5, Y622 in the first pore loop and F654 on S6. In addition, R696 in the TRP domain forms a cation-p interaction with W433 on pre-S1 while F590 on S5 and L673 on S6 form a CH-p interaction (Figure 1).

Third, H-bonds emerge between different hydrophilic residues. These H-bonding pairs are T397 and K432 on pre-S1 or E704 in the TRP domain, Q529 on S3 and Y448 or Y451 on S1, T566 on S4 and S576 in the S4-S5 linker, R567 on S4 and T699 in the TRP domain, Q570 in the S4-S5 linker and E689 in the TRP domain, D586 on S5 and T680 on S6, Y594 on S5 and Y661 on S6, E679 and N683 on S6. In addition, the vanilloid site phosphatidylcholine (PC) also relates W521 on S3 to Q580 in the S4-S5 linker via H-bonds. Of special note, there are several H-bonds between E610 and K614 in the first pore loop, S621 in the first pore loop and Q646 in the second pore loop, S624 and D627 in the first pore loop, T636 on the

pore helix and Y594 on S5 or Y661 on S6, N647 in the second pore loop and E610 or K614 in the first pore loop (Figure 1).

Taken together, one largest hairpin with a 23-residue loop is present to control the D519-R416 salt bridge in the VSLD/pre-S1 interface. It starts with R416 to W433, F441, Y565, F445, F449, Y448 and ends with F526. The total numbers of all non-covalent interactions and hairpin sizes along the gating pathway from D396 to K705 are 44 and 117, respectively (Figure 1).

2.2. The Largest Hairpin Melts to Initiate a Temperature Threshold 42□C for Oxidized mTRPV3 Activation

In the heat-activated sensitized state at 42□C, oxidized mTRPV3 has several changes. In the pore domain, the H-bonds between N647 and E610 or K614, S621 and Q646, S624 and D627, E679 and N683 are broken while the S620-Q646 H-bond emerges. In the S4-S5 linker/TRP interface, the Q570-E689 H-bond is disconnected. In the TRP domain and its interfaces with the pore domain and the pre-S1 domain, the E682-K686 and E689-R693 salt bridges are replaced with the N683-K686 and E689-R693 H-bonds, respectively. In addition, the T397-K432/E704 H-bonds are disrupted while the E405-K705 salt bridge and the E423-T427 and E418-R690 H-bonds are present. In the VSLD and its interface with the pre-S1 domain, the p-p interactions shifts from F445-Y565 and W493-Y451 to F526-Y565 and F489-F450, respectively, with the broken W493-F489 p-p interaction. The D519-R416 salt bridge is substituted by the S511-N412 and R509-N410 H-bonds. Of special interest, in the VSLD/S4-S5 linker interface, the T566-S576 H-bond is broken. However, D519 forms a salt bridge with R567 when a vanilloid site PC in the closed state disappears [18] (Figure 2).

Together, after the largest hairpin with a 23-residue loop in the VSLD/pre-S1 interface melts, two largest hairpins follow. One has a 9-residue loop in the pore domain starting with S620 and through Y622 and F654 and ending with Q646. The other contains an 8-residue loop from D519 to F526, Y565 and R567 in the VSLD/S4-S5 linker interface. The total numbers of all non-covalent interactions and hairpin sizes along the gating pathway from D396 to K705 become 41 and 87, respectively (Figure 2).

2.3. Two Smaller Hairpins in the S4-S5 Linker/VSLD Interface Are Required to Open Oxidized mTRPV3

When oxidized mTRPV3 is finally open from the sensitized state, there are small changes in the outer pore loop. The E610-K614/D615 H-bonds are replaced with the K616-D618 salt bridge. The D586-K589 salt bridge is disconnected while the S624-D627 H-bond is restored. In the meanwhile, a CH-p interaction is present between Q646 and F654, producing the smallest hairpin with a 1-residue loop from S620 to Y622 and F654 and Q646. Thus, the largest hairpin appears in the pore domain with a 10-residue loop from D586 to F590 and L673 and T580 and back to D586 (Figure 3).

In stark contrast, in the TRP domain and its interface with the pre-S1 domain, the E687-R690 and E405-K705 salt bridges and the T397-E704 H-bond are broken. In the meantime, the E689-R693 H-bond becomes a salt bridge and T411 forms a new H-bond with R416. In the VSLD/pre-S1 interface, the N410-R509 and N412-S511 H-bonds are replaced with the T411-S515 and N412-Q514 ones. In the VSLD, the p-

p interaction shifts from F450-F489 to Y451-W493. The H477-Y540 H-bond and the H471-Y547 p-p interaction also produce a new small hairpin with a 5-residue loop. When the T566-S576 H-bond is reinstated in the S4-S5 linker/VSLD interface, the resultant second largest hairpin with a 9-residue loop, together with an 8-residue loop from D519 to F526 and Y564 and Y565 and R567 and then back to D519, may be required for mTRPV3 opening. By all accounts, in the open state, the total numbers of all non-covalent interactions and hairpin sizes along the gating pathway from D396 to K705 become 41 and 71, respectively (Figure 3).

2.4. Reduced mTRPV3 Has the Different Largest Hairpin in the Outer Pore

In the closed state without the C612-C619 disulfide bond, reduced mTRPV3 is different than oxidized one. In the pore domain, the D586-T680, E610-K614, S621-Q646, S624-D627 and N647-E610/K614 H-bonds are disrupted together with the F590-L673 and Y622-F654 CH/p-p interactions and the E631-K634 salt bridge. In the meanwhile, the S613-N647 and E631-N643 H-bonds and the F625-V629 and N647-F654 CH-p interactions are formed. By all accounts, the largest hairpin with a 17-residue loop in the pore domain is born from S613 to F625, V629, E631, N643, N647, and then back to S613 (Figure 4).

However, the largest hairpin in the VSLD/pre-S1 interface, which is present in the oxidized mTRPV3 (Figure 1), is unavailable because the D519-R416 salt bridge has been replaced with the new Q514-T411/N412 H-bonds to produce the smallest hairpin with no residue in the loop. When the Y451-W493 p-p interaction is disconnected with the formation of the K500-E702 salt bridge, a smaller hairpin with a 9-residue loop is present from W493 to K500, E702, R698, R696, W433, F441, Y565, Y448, F447 and then back to W493. In the S4-S5 linker/TRP interface, the R567-T699 H-bond is substituted by the R567-Q695 H-bond. In the S4-S5 linker/pore domain interface, the D586-T680 H-bond is replaced with the K581-E687 salt bridge. In the TRP domain and its interface with the pre-S1 domain, the E687-R690 salt bridge is substituted by the 693-H426 H-bond. In the closed state, reduced mTRPV3's total numbers of all non-covalent interactions and hairpin sizes along the gating pathway from D396 to K705 are 40 and 96, respectively (Figure 4).

2.5 2-APB Can Open Reduced mTRPV3 at Low Temperature without Significant Changes in the Largest Hairpin Size and the Total Hairpin Sizes along the Gating Pathway

When one 2-APB agonist binds between F526 and S444 and the other between W433 and W692 via CH/p-p interactions (Figure 5), reduced mTRPV3 is open with several changes. In the VSLD, the Y565-F445/Y448 and Y540-Y547 p-p interactions are replaced with the F447-F489 and H471-Y540/Y547 ones and the S511-S515 H-bond. In the VSLD/TRP interface, the K500-E702 salt bridge is disconnected. In the S4-S5 linker/VSLD interface, the T566-S576 H-bond appears again. In the S4-S5 linker/TRP interface, Q570 also forms an H-bond with R693. In the TRP domain, the E679-N683 H-bond is disrupted. When these conformational changes are extended to the outer pore loop, the S613-N647 H-bond is broken. In the meanwhile, the E610-S624 H-bond, the E631-K634 salt bridge and the L605-F654 and F625-V629 CH-p interactions are born. However, the largest hairpin size still has 17 residues in the loop from Y594 to L605, F654, Y661 and then back to Y594. In addition to the smaller hairpin with a 9-residue loop from

T566 to S576, another with no residue in the loop from Q570 to E689 and R693 and then back to Q570 in the S4-S5 linker/TRP interface may be required to stabilize the 2-APB efficacy. In any way, the total numbers of all non-covalent interactions and hairpin sizes along the gating pathway from D396 to K705 become 44 and 99, respectively (Figures 4-5).

3. Discussion

The DNA hairpin biosensor employs oligonucleotides with complementary nucleotide sequences at the ends to form a duplex region as the stem upon intra-strand hybridization, and the nucleotides in between as the loop. The DNA hairpin melts above a temperature threshold. However, both opening and closure of the hairpin coexist at a threshold. With constant H-bonded base pairs in the stem and given ionic strengths in a solution, the threshold can be increased more than 20 degrees if the loop size is lowered down from 20 to 10 bases [17].

Although protein and DNA use sequences of amino acids and nucleotides to form primary polypeptide and polynucleotide chains, respectively, a change in the loop sequence has no significant effect on the melting temperature of the DNA hairpin [17]. Therefore, when an intramolecular non-covalent interaction creates a topological hairpin loop, the loop is thermodynamically equivalent between DNA and protein and thus can be applied to reveal the origin of the temperature threshold and sensitivity of thermo-gated TRPV3.

At the temperature threshold 42□C, closed mTRPV3 in the presence of the C612-C619 disulfide bond has the largest hairpin with a 23-residue loop from D519 to F526, Y448, Y565, F441, W433 and R416 to govern the VSLD/pre-S1 interface via the D519-R416 salt bridge (Figure 1). It melts in both sensitized and open states when D519 forms the critical salt bridge with R567 in the S4-S5 linker/VSLD interface (Figures 2-3). In the meanwhile, the new largest hairpin has a 10-residue loop in the pore domain. However, when this disulfide bond is disrupted, reduced mTRPV3 cannot open at 42□C [24], possibly because the melting of the largest hairpin with a 17-residue loop in the outer pore needs a higher temperature threshold above 50□C (Figure 4) [17]. In contrast, the largest hairpin always has 17 residues in the loop even if 2-APB opens reduced mTRPV3 (Figure 6). Therefore, the largest hairpin along the gating pathway may determine the temperature threshold of thermo-gated mTRPV3 [18].

When oxidized mTRPV3 opens at 42□C [18], the total number of all hairpin sizes along the gating pathway from D396 on pre-S1 to K706 in the TRP domain decreases from 117 to 71 residues. In contrast, when 2-APB opens reduced mTRPV3 at 4□C [22], this value remains around 96 residues except that 2-APB binding increases 4 residues in the total hairpin sizes (Figure 6). Since a smaller hairpin has a higher melting temperature and thus a larger heat capacity [17], it is proposed that the higher temperature coefficient (Q_{10}=27) in mTRPV3 may result from the 46-residue decrease in the total hairpin loop sizes along the gating pathway. In addition, the release of a PC lipid at the vanilloid site for channel opening also contributes 1/5 to Q_{10} (Figures 1-3) [18].

When reduced mTRPV3 is activated and open at 52□C, the largest hairpin with a 17-residue loop in the pore may melt and C612 is close to C619 enough to produce a disulfide bond. When oxidized mTRPV3 closes the channel below 52□C, the largest hairpin is born with a 23-residue loop in the pre-S1/VSLD interface so that the second threshold decreases to 42□C for oxidized mTRPV3 opening [18] (Figure 6). In other words, the temperature threshold of mTRPV3 is redox-dependent.

In closed and sensitized and open states of mTRPV3, some non-covalent interactions are state- and redox-independent no matter whether the stimulus is physical or chemical. For example, the K432-E704/D396 and E689-R693 and R698-E702 salt bridges, the Y448/Y451-Q529 and Y594-T636/Y661 H-bonds, and the F441-W433/Y565 and Y526-Y448/Y564 and Y564-Y565 and F590-Y594 p-p interactions. Therefore, these non-covalent interactions and the related hairpin topological structures may form a basic stable backbone anchor system for thermoTRPV3 activation or a heat fuse group to prevent heat denaturation [18, 22]. On the other hand, several smaller hairpins may be required for heat-evoked TRPV3 opening (Figure 6B).

The first has no residue in the loop from Y594 to T636 and Y661 and back to Y594 (Figure 6B). In support of this notion, the mutation N643S, I644S, N647Y, L657I, or Y661C in the outer pore is less sensitive to heat [25], possibly because those mutations may destablize that smallest hairpin and thus decrease the heat efficacy (Figures 1-3).

The second has a 10-residue loop from D586 to F590, L673 and T680 and then back to D586 (Figure 3A). In agreement with this proposal, the T680A mutation suppresses the heat-evoked opening of reduced mTRPV3 with the N-terminal 1–117 residues truncated [26].

The third has no residue in the loop from T411 to N412 and Q514 and then back to T411 (Figure 6B). However, when the insertion of valine or serine at position 412 disrupts the Q514-N412 H-bond, another hairpin with a loop size larger than 17 residues may be formed in the VSLD/pre-S1 interface and thus dramatically decrease the threshold and sensitivity [27].

The fourth has no residue in the loop from Y448 to F526, Y564, Y565 and back to Y448 (Figure 6B). It has been reported that the Y564A mutation decreases the threshold of reduced mTRPV3 from 52□C to 37□C and the temperature sensitivity [24].

Finally, further experiments are necessary to test if non-covalent interactions in other smaller hairpins are essential for heat-evoked TRPV3 opening. For example, the D519-R567 salt bridge, the T566-S576 and R567-Q695 and S622-Q646 H-bonds, the Y622-F654 and F441-Y565 and Y448-F526/Y565 p-p interactions, and the R696-W433 cation-p interaction (Figures 2A, 3A, 6B).

4. Online Methods

In this *in silicon* study, the cryo-EM structural data of oxized mTRPV3 with a high resolution in different gating states at 42□C were analyzed with graph theory to reveal the roles of the hairpin topological loop

sizes in regulating the temperature threold and the thermosensitivity of TRPV3. They include closed mTRPV3 in cNW11 (PDB ID, 7MIN, model resolution= 3.09 Å) and MSP2N2 (PDB ID, 7MIK, model resolution= 3.12 Å), sensitized mTRPV3 in MSP2N2 (PDB ID, 7MIL, model resolution= 3.86 Å), and open mTRPV3 in cNW11 (PDB ID, 7MIO, model resolution= 3.48 Å) [18]. In addition, the cryo-EM structural data of detergent-solubilized reduced mTRPV3 with (PDB ID, 6DVY, model resolution= 4.0 Å) and without (PDB ID, 6DVW, model resolution= 4.3 Å) 2-APB bound at 4□C were also analyzed as controls to reveal the origin of the temperature threold and the thermosensitivity of TRPV3 [22].

Structure visualization software, UCSF Chimera, was used to assess the presence of non-covalent interactions in TRPV3. Since the gating of thermoTRP channels is governed by stereo- or regioselective inter- or intradomain interactions, only stereo- or regioselective diagonal and lateral non-covalent interactions were included in this study to test their potential roles in forming hairpin topological loops to control the temperature threshold and sensitivity. They included, but are not limited to, salt-bridges, CH/cation/p-p interactions and H-bonds along the gating pathway in mTRPV3 with or without 2-APB bound. In contrast, the hydrophobic interactions were not considered because they lack both stereo- and regio-selectivity [28].

The standard definition of noncovalent interactions was employed. A hydrogen bond was considered present when the angle donor-hydrogen-acceptor is within the cut-off of 60°, and when the hydrogen-acceptor distance is within 2.5 Å and the maximum distance is 3.9 Å between a donor and an acceptor. A salt bridge was considered to be formed if the distance between any of the oxygen atoms of acidic residues and the nitrogen atoms of basic residues are within the cut-off distance of 3.2-4 Å in at least one frame. When the geometry is acceptable, a salt bridge is also counted as a hydrogen bonding pair. The face-to-face π-π stacking of two aromatic rings was considered effective once the separation between the π-π planes is ~3.35-4.4 Å, which is close to at least twice the estimated van der Waals radius of carbon (1.7Å). The edge-to-face π-π interaction of two aromatic rings was considered attractive when the cut-off distance between two aromatic centers is within 4-6.5 Å. Significant cation- π interactions occur within a distance of 6.0 Å between a cation and an aromatic center. The short effective CH/π distances is 2.65-3.01 Å between aromatic groups, and 2.75-2.89 Å between CH_3 and an aromatic ring. The lone pair-π interaction distance between a lone electron pair and an aromatic ring is within 3-3.7 Å.

After non-covalent interactions were scanned along the gating pathway of mTRPV3, graph theory was used to define the minimum hairpin topological loop size to control every non-covalent interaction and geometrically to realize the hairpin topological loop maps along the gating pathway from D396 in the pre-S1 domain to K705 in the TRP domain in the closed, sensitized or open states at 4□C and 42□C. The primary amino acid sequence line from D396 to K705 was marked in black. An amino acid side chain involving a non-covalent interaction along the gating pathway of mTRPV3 was defined as a vertex and marked with an arrow in different colors. The same kind of non-covalent interactions between two amino acid side chains was marked with an edge in the same color. A hairpin topologicval loop was considered significant when an edge forms a sealed topological ring with the amino acid sequence between two ends of the edge or other edges. If n was the sum of the sequence number differences between two

adjacent vertexes in a hairpin topologcal loop, the loop size was defined as (n-1). The minimum hairpin topological loop to control the thermostability of a non-covalent interactrion was definded with the least product of the number of non-covalent interactions in the loop and the loop size. Only the minimum hairpin topological loop sizes were marked in black. The largest or gating hairpin sizes were shown in a red circle. The total number of all noncovalent interactions and hairpin sizes along the gating pathway were shown in black and blue circles, respectively.

Q_{10} was used to characterize the temperature-dependent responses of DNA hairpins and thermoTRP channels as calculated using the following equation:

$$Q_{10} = (R2/R1)^{10/(T2-T1)}$$

where, R1 and R2 are rates of a reaction at two different temperatures T1 and T2 in Celsius degrees or kelvin, respectively.

Abbreviations

ARD, ankyrin repeat domain; 2-APB, 2-aminoethoxydiphenyl borate; cryo-EM, cryo-electron microscopy; PC, phosphatidylcholine; TMD, transmembrane domain; TRP, transient receptor potential; TRPV3, TRP vanilloid-3; mTRPV3, mouse TRPV3; VSLD, voltage-sensor-like domain.

Declarations

Acknowledgements

The author's own studies cited in this article were supported by NIDDK Grant (DK45880 to D.C.D.) and Cystic Fibrosis Foundation grant (DAWSON0210) and NIDDK grant (2R56DK056796-10) and American Heart Association (AHA) Grant (10SDG4120011 to GW).

Conflict of Interest: The author declares no conflict of interest.

Data Availability Section: This study includes no data deposited in external repositories.

References

1. Caterina, M.J., Schumacher M.A., Tominaga M., Rosen T.A, Levine J.D. and Julius D. The capsaicin receptor: a heat-activated ion channel in the pain pathway. *Nature*. **1997**. 389(6653), 816-824.
2. Caterina, M.J., Rosen T. A., Tominaga M., Brake A. J, Julius D. A capsaicin-receptor homologue with a high threshold for noxious heat. *Nature* **1999**, 398,436.
3. McKemy D. D., Neuhausser W. M. & Julius D. Identification of a cold receptor reveals a general role for TRP channels in thermosensation. *Nature***2002**; 416(6876), 52–58.

4. Peier, A.M., Moqrich A., Hergarden A.C., Reeve A.J., Andersson D.A., Story G.M., Earley T.J., Dragoni I., McIntyre P., Bevan S. and Patapoutian A. A TRP channel that senses cold stimuli and menthol. *Cell*. **2002a**; 108(5), 705–715.
5. Peier A. M., Reeve A. J., Andersson D.A., Moqrich A., Earley T.J., Hergarden A.C., Story G.M., Colley S., Hogenesch J. B., McIntyre P., Bevan S., Patapoutian A. A heat-sensitive TRP channel expressed in keratinocytes. *Science*. **2002b,** 296, 2046.
6. Smith G. D., Gunthorpe M. J., Kelsell R. E., Hayes P. D., Reilly P., Facer P., Wright J. E., Jerman J. C., Walhin J-P., Ooi L., Egerton J., Charles K. J., Smart D., Randall A. D., Anand P., Davis J. B. TRPV3 is a temperature-sensitive vanilloid receptor-like protein. *Nature***2002**, 418, 186.
7. Xu H., Ramsey I. S., Kotecha S. A., Moran M. M., Chong J. A., Lawson D., Ge P., Lilly J., Silos-Santiago I., Xie Y., DiStefano P. S., Curtis R., Clapham D. E. TRPV3 is a calcium-permeable temperature-sensitive cation channel. *Nature***2002**, 418, 181.
8. Guler A.D., Lee H., Iida T., Shimizu I., Tominaga M.and Caterina M. J. Heat-evoked activation of the ion channel, TRPV4. *J Neurosci***2002**, 22, 6408–14.
9. Chung M. K., Lee H., Caterina M. J. Warm temperatures activate TRPV4 in mouse 308 keratinocytes. *J. Biol. Chem*. **2003**, 278, 32037.
10. Story, G.M., Peier A.M., Reeve A.J., Eid S.R., Mosbacher J., Hricik T.R., Earley T.J., Hergarden A.C., Andersson D.A., Hwang S.W., McIntyre P., Jegla T., Bevan S., Patapoutian A. ANKTM1, a TRP-like channel expressed in nociceptive neurons, is activated by cold temperatures. *Cell*. **2003**, 112, 819–829.
11. Jordt, S.E., Bautista D.M., Chuang H.H., McKemy D.D., Zygmunt P.M., Högestätt E.D., Meng I.D. and Julius D. Mustard oils and cannabinoids excite sensory nerve fibres through the TRP channel ANKTM1.*Nature.***2004**, 427, 260–265.
12. Talavera K, Yasumatsu K., Voets T., Droogmans G., Shigemura N., Ninomiya Y., Margolskee R. F., Nilius B. Heat activation of TRPM5 underlies thermal sensitivity of sweet taste. *Nature***2005**, 438, 1022.
13. Vriens J, Owsianik G., Hofmann T., Philipp S., Stab J., Chen X., Benoit M., Xue F., Janssens A., Kerselaers S., Oberwinkler J., Vennekens R., Gudermann T., Nilius B., Voets T. TRPM3 is a nociceptor channel involved in the detection of noxious heat. *Neuron***2011**, 70, 482.
14. Zimmermann,K., Lennerz J.K., Hein A., Link A.S., Kaczmarek J.S., Delling M., Uysal S., Pfeifer J.D., Riccio A. and Clapham D.E. Transient receptor potential cation channel, subfamily C, member 5 (TRPC5) is a cold-transducer in the peripheral nervous system. *Proc. Natl. Acad. Sci.USA*. **2011**, 108, 18114–18119.
15. Song K., Wang H., Kamm G. B., Pohle J., Reis F. C., Heppenstall P., Wende H., Siemens J.. The TRPM2 channel is a hypothalamic heat sensor that limits fever and can drive hypothermia. *Science***2016**, 353,1393.
16. Tan C. H., McNaughton P. A. The TRPM2 ion channel is required for sensitivity to warmth. *Nature***2016**, 536, 460.

17. Jonstrup A.T., Fredsøe J., Andersen A.H. DNA Hairpins as Temperature Switches, Thermometers and Ionic Detectors. *Sensors* **2013**, 13, 5937-5944.
18. Nadezhdin, K. D., Neuberger, A., Trofimov, Y. A., Krylov, N. A., Sinica, V., Kupko, N., Vlachova, V., Zakharian, E., Efremov, R. G., and Sobo-levsky, A. I. Structural mechanism of heat-induced opening of a temperature-sensitive TRP channel. *Nat. Struct. Mol. Biol*. **2021,** 28, 564–572.
19. Liao M, Cao E., Julius D. & Cheng Y. Structure of the TRPV1 ion channel determined by electron cryo-microscopy. *Nature***2013**, 504,107.
20. Liu B.Y., Yao J., Zhu M.X. & Qin F. Hysteresis of gating underlines sensitization of TRPV3 channels. *J. Gen. Physiol.***2011**, 138, 509–520.
21. Liu B. & Qin F. Use dependence of heat sensitivity of vanilloid receptor TRPV2. *Biophys J***2016**, 110(7), 1523–1537.
22. Singh, A.K., McGoldrick L.L. and Sobolevsky A.I. Structure and gating mechanism of the transient receptor potential channel TRPV3. *Nat. Struct. Mol. Biol.***2018**, 25, 805–813
23. Zubcevic, L., Herzik Jr. M. A., Wu M., Borschel W.F., Hirschi M., Song A.S., Lander G.C., and Lee S. Y. Conformational ensemble of the human TRPV3 ion channel. *Nat. Commun.***2018**, 9, 4773.
24. Singh, A.K., McGoldrick L.L., Demirkhanyan L., Leslie M., Zakharian E., and Sobolevsky A.I. Structural basis of temperature sensation by the TRP channel TRPV3. *Nat. Struct.Mol. Biol.***2019**, 26, 994–998.
25. Grandl JH, Hu H, Bandell M, Bursulaya B, Schmidt M, Petrus M and Patapoutian A. Pore region of TRPV3 ion channel is specifically required for heat activation. *Nat. Neurosci*. **2008**, 11, 1007–1013.
26. Shimada, H., Kusakizako, T., Nguyen, THD, Nishizawa, T., Hino T., Tominaga M., Nureki, O. The structure of lipid nanodisc-reconstituted TRPV3 reveals the gating mechanism. *Nat Struct Mol Biol.***2020,** 27, 645-652.
27. Liu, B. & Qin F. Single-residue molecular switch for high-temperature dependence of vanilloid receptor TRPV3. *Proc. Natl.Acad. Sci. USA.***2017**, 114, 1589–1594.
28. Baumgartner A. Insertion and Hairpin Formation of Membrane Proteins: A Monte Carlo Study. **1996,***Biophys. J.* 71, 1248-1255.

Figures

Figure 1

The hairpin topological structures along the gating pathway of oxidized mTRPV3 in the closed state at 42□C. **A,** Amino acids side chains for salt bridges or H-bonds or cation/CH/p-p interactions along the gating pathway from D396 to K705. The cryo-EM structure of apo mTRPV3 in cNW11 (PDB ID, 7MIN) was used for the model [18]. The residues are colored in red for a positive charge or blue for a negative charge or orange for the uncharged residues in salt bridges or H-bonds or cation/CH/p-p interactions, and green

for p interactions. The PC lipid site and the largest hairpin with a 23-residue loop in the VSLD/pre-S1 interface are shown in the right two panels. **B**, The hairpin topological loops map. The pore domain, the S4-S5 linker, the TRP domain, the VSLD and the pre-S1 domain are indicated in black. Salt bridges, p interactions, and H-bonds between amino acid side chains along the gating pathway from D396 to K705 are marked in purple, green, and orange, respectively. The minimum hairpin topological loop sizes required to control the relevant non-covalent interactions are labeled in black. The total numbers of all hairpin loop sizes and non-covalent interactions along the gating pathway are shown in the blue and black circles, respectively.

Figure 2

The hairpin topological structures along the gating pathway of oxidized mTRPV3 in the heat-activated sensitized state at 42□C. **A,** Amino acids side chains for salt bridges or H-bonds or cation/CH/p-p interactions along the gating pathway from D396 to K705. The cryo-EM structure of mTRPV3 in MSP2N (PDB ID, 7MIL) was used for the model [18]. The residues are colored in red for a positive charge or blue for a negative charge or orange for the uncharged residues in salt bridges or H-bonds or cation/CH/p-p interactions, and green for p interactions. The first and second largest hairpins with 9 and 8-residue loops are shown in the right panel, respectively. **B**, The hairpin topological loops map. The pore domain, the S4-S5 linker, the TRP domain, the VSLD and the pre-S1 domain are indicated in black. Salt bridges, p interactions and H-bonds between amino acid side chains along the gating pathway from D396 to K705 are marked in purple, green and orange, respectively. The minimum hairpin topological loop sizes required to control the relevant non-covalent interactions are labeled in black. The total numbers of all hairpin loop sizes and non-covalent interactions along the gating pathway are shown in the blue and black circles, respectively.

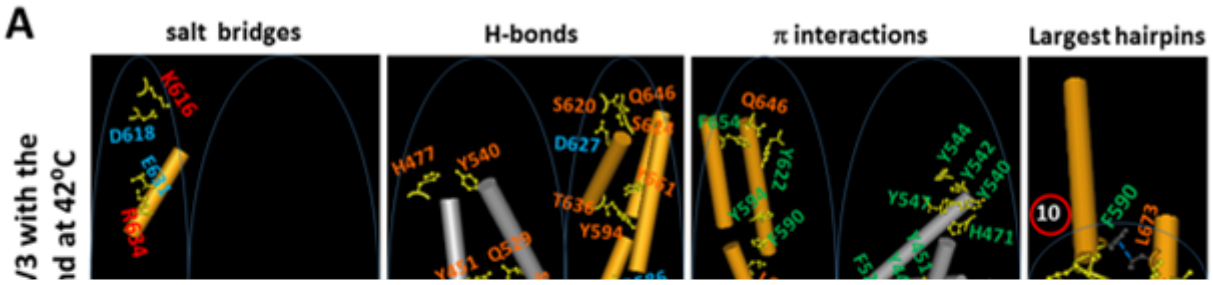

Figure 3

The hairpin topological structures along the gating pathway of oxidized mTRPV3 in the open state at 42□C. **A,** Amino acids side chains for salt bridges or H-bonds or cation/CH/p-p interactions along the gating pathway from D396 to K705. The cryo-EM structure of apo mTRPV3 in cNW11 (PDB ID, 7MIO) was used for the model [18]. The residues are colored in red for a positive charge or blue for a negative charge or orange for the uncharged residues in salt bridges or H-bonds or cation/CH/p-p interactions, and green for p interactions. The first and second largest hairpins with 10 and 9-residue loops are shown in the right panel, respectively. **B**, The hairpin topological loops map. The pore domain, the S4-S5 linker, the TRP domain, the VSLD and the pre-S1 domain are indicated in black. Salt bridges, p interactions and H-bonds

between amino acid side chains along the gating pathway from D396 to K705 are marked in purple, green and orange, respectively. The minimum hairpin topological loop sizes required to control the relevant non-covalent interactions are labeled in black. The total numbers of all hairpin loop sizes and non-covalent interactions along the gating pathway are shown in the blue and black circles, respectively.

Figure 4

The hairpin topological structures along the gating pathway of reduced mTRPV3 in the closed state at 4□C. **A,** Amino acids side chains for salt bridges or H-bonds or cation/CH/p-p interactions along the gating pathway from D396 to K705. The cryo-EM structure of apo detergent-solubilzed mTRPV3 (PDB ID, 6DVW) was used for the model [22]. The residues are colored in red for a positive charge or blue for a negative charge or orange for the uncharged residues in salt bridges or H-bonds or cation/CH/p-p interactions, and slight green for p interactions. The largest hairpin with a 17-residue loop is shown in the right panel. **B**, The hairpin topological loops map. The pore domain, the S4-S5 linker, the TRP domain, the VSLD and the pre-S1 domain are indicated in black. Salt bridges, p interactions and H-bonds between amino acid side chains along the gating pathway from D396 to K705 are marked in purple, green and orange, respectively. The minimum hairpin topological loop sizes required to control the relevant non-covalent interactions are labeled in black. The total numbers of all hairpin loop sizes and non-covalent interactions along the gating pathway are shown in the blue and black circles, respectively.

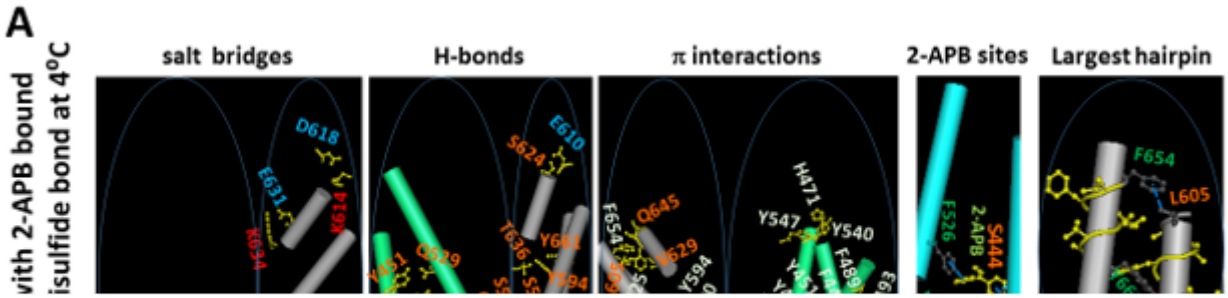

Figure 5

The hairpin topological structures along the gating pathway of reduced mTRPV3 with 2-APB in the open state at 4□C. **A,** Amino acids side chains for salt bridges or H-bonds or cation/CH/p-p interactions along the gating pathway from D396 to K705. The cryo-EM structure of detergent-solubilized mTRPV3 with 2-APB bound (PDB ID, 6DVY) was used for the model [22]. The residues are colored in red for a positive charge or blue for a negative charge or orange for the uncharged residues in salt bridges or H-bonds or cation/CH/p-p interactions, and slight green for p interactions. The two 2-APB sites and the largest hairpin with a 17-residue loop are shown in the right two panels. **B**, The hairpin topological loops map. The pore domain, the S4-S5 linker, the TRP domain, the VSLD and the pre-S1 domain are indicated in

black. Salt bridges, p interactions and H-bonds between amino acid side chains along the gating pathway from D396 to K705 are marked in purple, green and orange, respectively. The minimum hairpin topological loop sizes required to control the relevant non-covalent interactions are labeled in black. The total numbers of all hairpin loop sizes and non-covalent interactions along the gating pathway are shown in the blue and black circles, respectively.

Figure 6

The tentative model for the redox-dependent temperature threshold and sensitivity of thermo-gated TRPV3. **A.** The cryo-EM structures of mTRPV3 with or without 2-APB in the presence or absence of the C612-C619 disulfide bond (PDB ID: 6DVY, 6DVW,7MIN, 7MIO) were used for the model [18, 22]. In the absence of the C612-C619 disulfide bond, reduced mTRPV3 can be opened by 2-APB at 4□C. However, the largest hairpin size and the total number of all hairpin sizes along the gating pathway from D396 to K705 have not significant changes. When the temperature increases above 52□C, mTRPV3 is open upon the decrease of the larest hairpin size in the pore domain from 17 to 10 residues in the loops. The total number of all hairpin sizes along the gating pathway from D396 to K705 also decreases from 96 to 71 residues. In the meantime, C612 is close to C619 enough to form a disulfide bond. When the temperature decreases below 42□C, oxidized mTEPV3 is closed with a lower threshold as a result of the formation of a 23-residue loop as the largest hairpin in the VSLD/pre-S1 interface. The total number of all hairpin sizes along the gating pathway from D396 to K705 increases to 117 residues. Of note, the total number of non-covalent interactions is around 42 along the gating pathway in both closed and open states. **B.** The proposed smaller gating hairpins for heat-activated opening of mTRPV3.